

Reproducibility in dual energy CT: the impact of a projection domain material decomposition method

V. Haase^{a,b}, F. Noo^c, K. Stierstorfer^a, A. Maier^b, and M. McNitt-Gray^d

^aSiemens Healthcare GmbH, Forchheim, Germany

^bDepartment of Computer Science, Friedrich-Alexander-Universität Erlangen-Nürnberg, Erlangen, Germany

^cDepartment of Radiology and Imaging Sciences, University of Utah, Salt Lake City, USA

^dDepartment of Radiology, David Geffen School of Medicine, University of California, Los Angeles, USA

ABSTRACT

Reproducibility of CT numbers represents an ongoing challenge, especially in clinical applications where exams are performed to assess disease progression or response to therapy. Dual energy CT (DECT) offers an opportunity for improved image quantification, but also presents unique issues. This work presents an initial phantom study that investigates reproducibility over time, across different scanners, and with regard to positioning of the phantom. Both an image domain and a projection data domain material decomposition method are used to create mono-energetic images from DECT data. The scanned object is the ACR CT accreditation phantom. Images were evaluated for reproducibility both inside the phantom inserts of module A as well as in regions between the inserts, where image artifacts are frequently visualized. The results demonstrate that artifacts are worse for off-centered positions. They also demonstrate that the data-based material decomposition provides comparable HU numbers within the inserts of interest like the image-based method, but provides substantially less artifacts and less HU variability in regions surrounding the inserts across the different phantom positions.

1. INTRODUCTION

Reproducibility of CT numbers represents an ongoing challenge, especially in clinical applications where exams are performed to assess disease progression or response to therapy. In these exams, comparison to a baseline or previous exam is critical. When these applications involve quantitative assessments (e.g., lung nodule density, emphysema scoring), the reproducibility of HU across scans becomes critical. DECT offers an opportunity for improved image quantification, but also presents unique issues. Previously, we explored a projection data-based method for material decomposition that uses an analytical energy response model to create mono-energetic images from DECT data.¹ The purpose here is to investigate how well this method performs in terms of artifacts and HU variability in a phantom study. The investigation addresses two challenging conditions: 1) scan repetition on another scanner with a three-year time difference, 2) changes in the position and orientation of the phantom.

2. BACKGROUND

The methods to create mono-energetic images from DECT data can be grouped into two categories: image-based and data-based material decomposition approaches. In this work, we are comparing both approaches by using a specific realization of each of them which is shortly explained in this section.

For the image-based approach, the material decomposition takes place in the image domain, after the high and low energy projection data sets are separately reconstructed. Here, we use an image-based decomposition approach that follows the steps outlined in.² In short, two region of interests (ROIs) are selected, each of which only includes pixels from one of the two basis materials. For each kV setting, the mean attenuation value of both ROIs is computed, then their ratio is compared with a ground truth ratio to identify an effective energy for the

Acknowledgement: This project was partly supported by Siemens Healthcare GmbH and partly by the National Heart Lung and Blood Institute of the National Institutes of Health under R01HL153964-01. The concepts and information presented in this paper are based on research and are not commercially available. Its contents are solely the responsibility of the authors and do not represent the official views of the NIH.

scan. Once the effective energy is known for the high and low energy scans, the decomposition proceeds on a pixel-by-pixel basis by inversion of a 2×2 system of equations. The input groups the two pixel values observed from the high and low energy scans. The matrix assembles the linear attenuation coefficient (LAC) of each basis material at the effective energy of the high and low energy scans. The output gives the components along each basis material. Finally, the pixel value in the mono-energetic image is obtained by linearly combining the LAC of the two basis materials at the desired energy using the obtained components.

For the data-based approach, the material decomposition is performed directly from the projection data of the high and low energy scans. The outcome of the decomposition is the line integrals of the images whose pixel values are the components along each basis material. Image reconstruction is taking place after the decomposition and yields the components for each pixel. The final step to create the mono-energetic image is the same as in the image-based approach. In,¹ we proposed a data-based approach that uses an analytical energy response model for the CT system. In this work, we use the same method as it has shown robust results using real CT data.

3. EXPERIMENTAL SETUP

3.1 Baseline Experiments

We use module A of the ACR CT accreditation phantom (model 464, Gammex-RMI, USA). Module A is a cylinder of water-equivalent material with a diameter of 20 cm and a length of 4 cm. It contains five cylindrical inserts representing the X-ray attenuation behaviour of bone, polyethylene, acrylic, air, and water. The chemical composition characteristics of each material were provided by the phantom's manufacturer. In addition, the module shows horizontal ramps for slice thickness evaluation and four 1 mm diameter steel beads to center the module in the z -direction. In 2018, the phantom was scanned using a state-of-the-art CT system (SOMATOM Definition AS+, Siemens Healthineers). All scans consisted of 2304 projections at a fixed bed position using an in-plane flying focal spot. The detector coverage was defined by 736 channels and 60 rows with a row width of 0.6 mm. The dual energy scans were acquired sequentially, i.e., the high and low energy scans were performed consecutively, with the X-ray tube set to 120 kV and 300 mAs, and to 80 kV and 500 mAs, respectively. The phantom was placed so that the center of module A closely matches the center of the scan field of view (FOV). The scans were repeated ten times and then averaged to reduce noise in the data for easier image analysis.

The collected data was processed with both image-based and data-based material decomposition methods explained in Section 2. The decomposition used the water-equivalent and bone-equivalent materials that are used to create the water and bone inserts in the ACR phantom. An offline filtered backprojection implementation of the vendor's own reconstruction software was used for image reconstruction. A semi-smooth kernel (D40s) that is recommended for quantitative applications was systematically applied.

3.2 Experiments on Reproducibility

New scans were taken three years later, in 2021, using the exact same phantom with a different scanner (SOMATOM Definition Flash, Siemens Healthineers). The scan geometry was the same except for the bowtie filter material and the beam collimation, which was changed to 32 rows with a 1.2 mm row width, so that the energy response model used in the data-based decomposition needed to be adjusted. The phantom was scanned using three different positionings. The first one was the same as that used for the baseline scan, i.e., the phantom is centered in the scan FOV. The second one included a vertical shift of 4.8 cm up. The last one included a counterclockwise rotation of 45° together with a vertical shift of 4.8 cm.

All projection data was processed as described previously to create mono-energetic images with the image- and the data-based approaches. For non-centered positionings of the phantom, a shifted grid of pixels was used.

4. RESULTS

4.1 Baseline Results

Fig. 1 shows the reconstructions of the high and low energy scans used as baseline. Fig. 2 presents the mono-energetic images at 70 keV, as obtained with the image- and data-based decompositions. This energy was selected because it results in the lowest amount of noise in the images. The image-based decomposition leads to streak

artifacts originating from the metal beads and to a bright artifact between the bone and the air insert, which is not present in the data-based result. To convey the quality of the implemented material decomposition approaches, Table 1 compares the mean attenuation value within the inserts in the mono-energetic images of Fig. 2 against the corresponding ideal attenuation values.

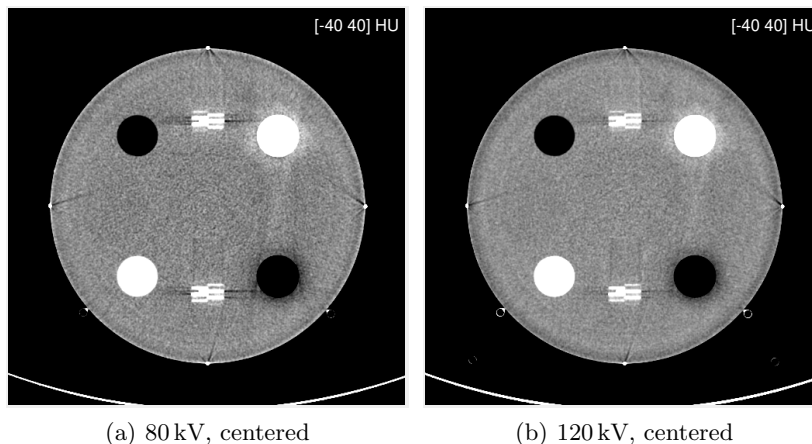


Figure 1. Reconstructed images of the baseline (a) low and (b) high energy scans.

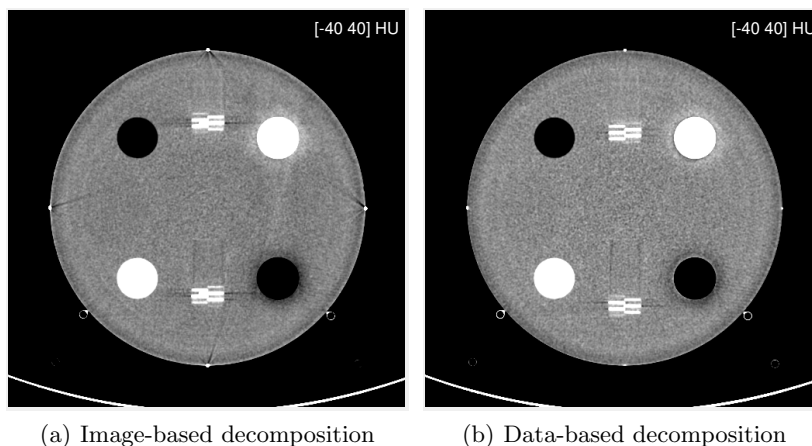


Figure 2. Mono-energetic images at 70 keV as computed from the baseline data, using (a) image-based and (b) data-based material decomposition.

Table 1. Mean linear attenuation values within the phantom’s inserts in cm^{-1} , as obtained at 70 keV using the baseline scan. Reference values given by NIST.³

# ROI: Material	Reference	Image-based	Data-based
1: Bone	0.3696	0.3735 ± 0.0000	0.3655 ± 0.0001
2: Polyethylene	0.1718	0.1756 ± 0.0000	0.1771 ± 0.0000
3: Acrylic	0.2172	0.2173 ± 0.0000	0.2184 ± 0.0000
4: Air	0.0002	0.0038 ± 0.0000	0.0035 ± 0.0000
5: Water	0.1916	0.1935 ± 0.0000	0.1935 ± 0.0000

4.2 Results on Reproducibility

Reconstructions of the new high and low energy scans in the centered, off-centered, and off-centered and rotated positionings are displayed in Fig. 3 as an initial guide to interpret the mono-energetic reproducibility results,

which are presented in Fig. 4. For the centered phantom, the images in Fig. 4 have an appearance similar to those from the baseline scans. When the phantom is moved out of the centered position, strong image artifacts around the bone insert can be observed in the image-based approach. These artifacts appear either absent or strongly reduced for the data-based approach.

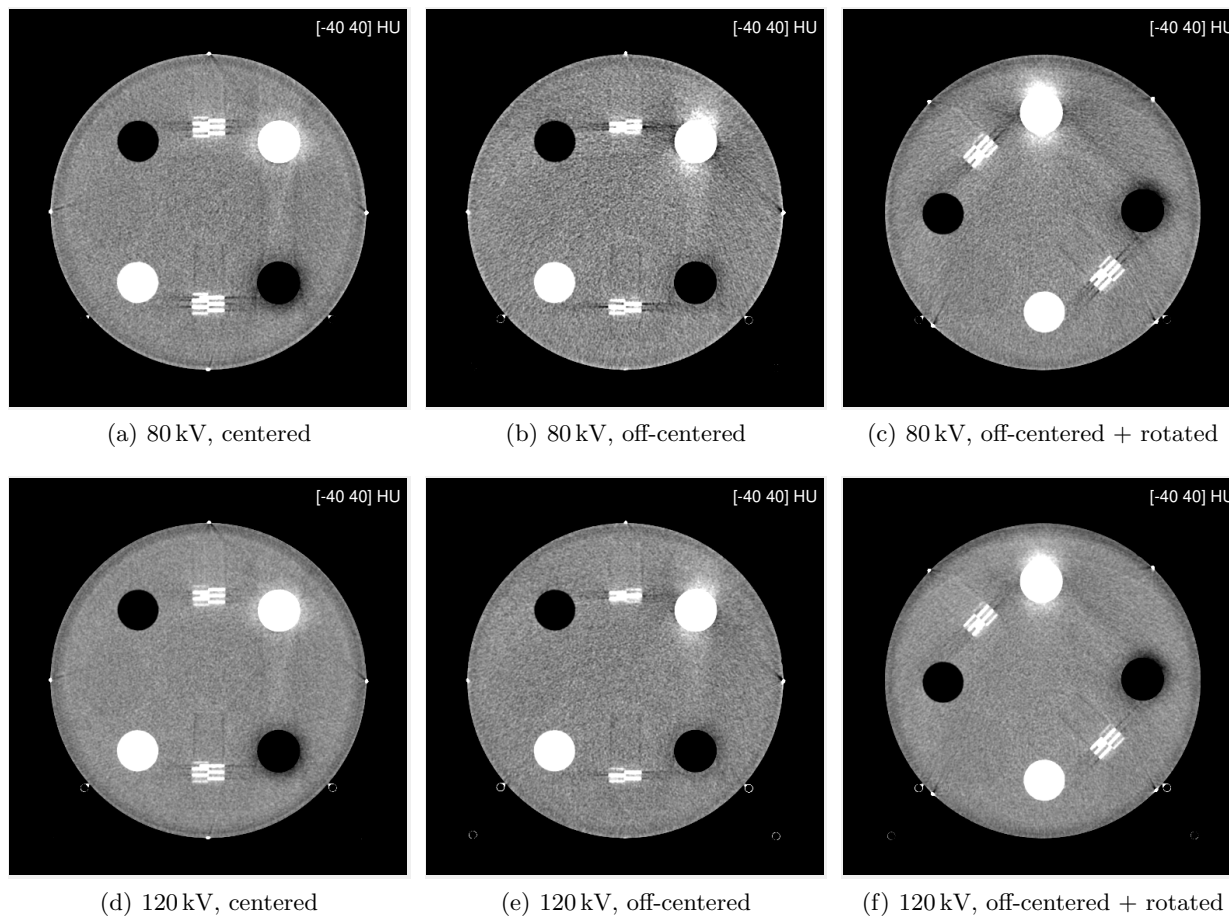


Figure 3. Reconstructed images for the new, high and low energy scans for the centered, off-centered, and off-centered and rotated positionings of the phantom.

For quantitative evaluation of the images in Fig. 4, Fig. 5 to Fig. 7 provide profile plots for differences with the baseline results. The mono-energetic images were registered to geometrically match the baseline results; the registration used cubic interpolation. Fig. 5 shows a circular profile around the bone insert, which was created by using 360 small ROIs around the bone insert, each with a radius of 5 pixels and placed at the same distance from the center of the bone insert. The differences in mean values for these ROIs are plotted starting at the 12 o'clock position going clockwise. The plots reveal more important deviations for the image-based approach than the data-based approach. For example, the image-based approach yields differences of -20 to 13 HU for the off-centered positioning of the phantom that only are of -6 to 5 HU when the decomposition is performed in the data domain. A second circular plot was created around the air insert in a similar manner as around the bone. Fig 6 shows that errors around the air insert are always in an acceptable range of -5 to 5 HU. It also shows that the results for the image-based approach are slightly better than for the data-based approach: for the off-centered positioning of the phantom, the curve for the data-based approach has a standard deviation of 2.03 HU while that for the image-based approach is 1.21 HU. A third profile plot is presented in Fig. 7, showing a thick horizontal profile, located below the bone insert within the main body of the phantom. Again, higher deviations from the baseline result can be observed when the image-based decomposition is used. We have also compared the mean values within the five inserts. The results (not shown here) convey that both image- and

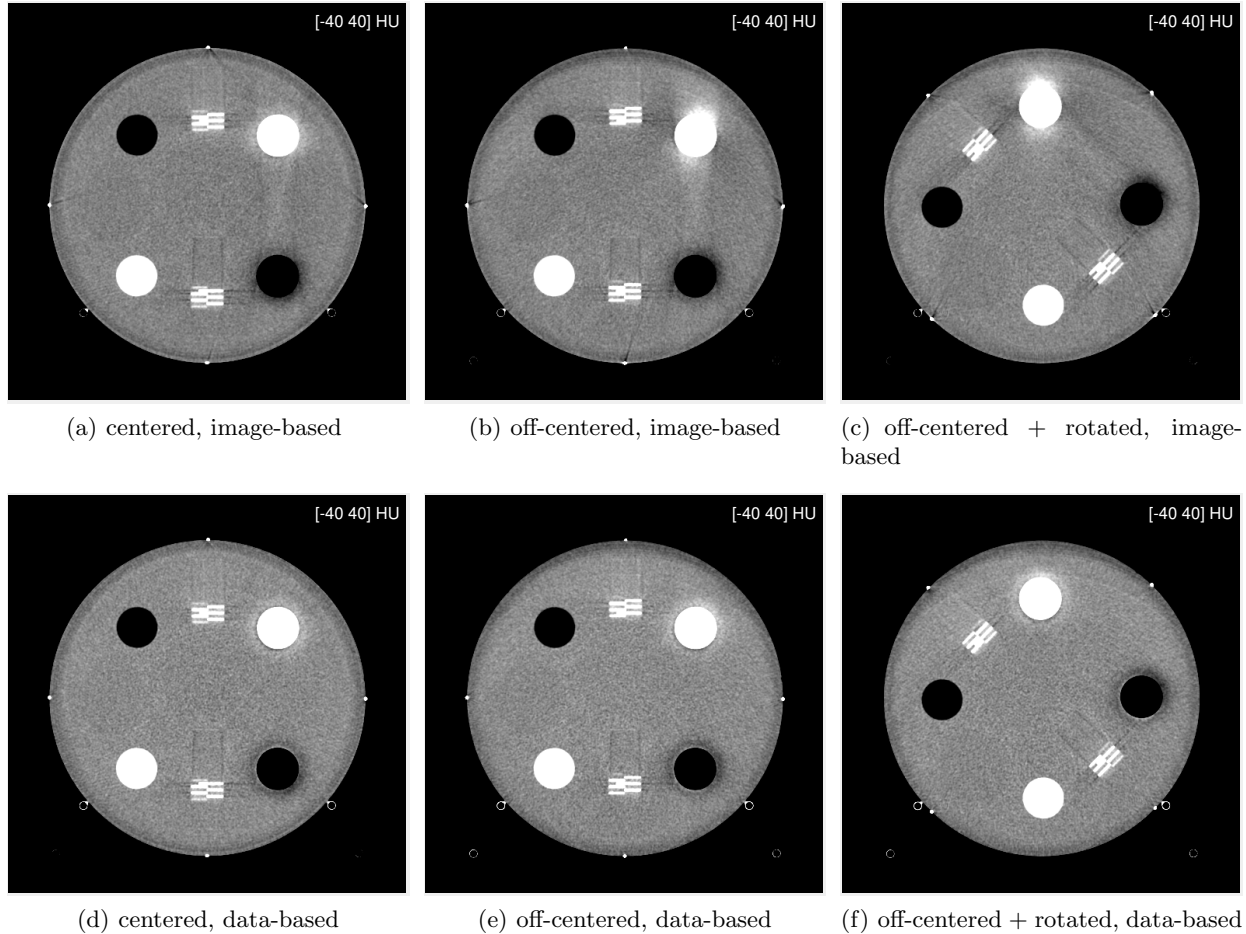


Figure 4. Mono-energetic images at 70 keV from the new scans: (left) image-based and (right) data-based material decomposition. Top to bottom: centered, off-centered, and off-centered and rotated positionings of the phantom.

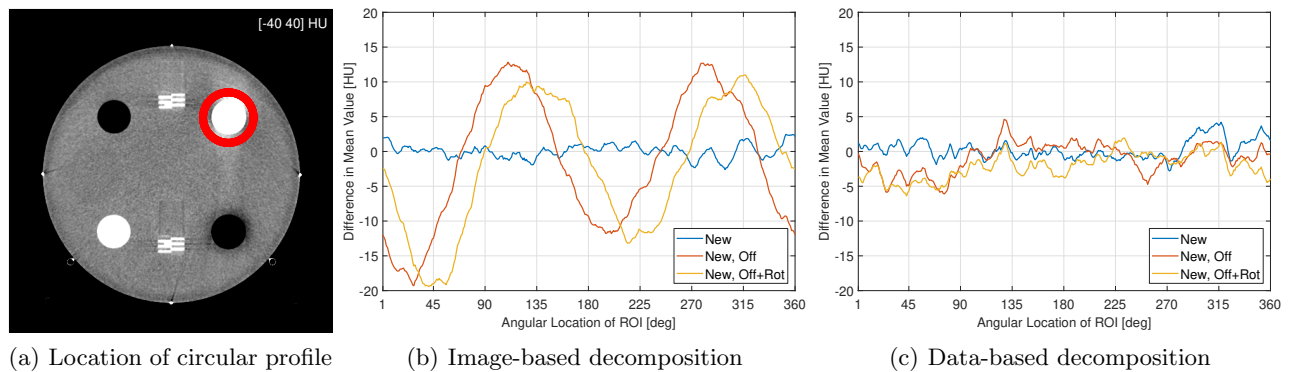
the data-based decomposition yields similar accuracy, with all absolute differences less than 5.0 HU.

5. DISCUSSION AND CONCLUSION

We presented an initial phantom study investigating artifacts and reproducibility in HU that result from applying a method we previously presented for DECT with material decomposition in the data domain. The investigation included changes over time and scanner, as well changes in phantom positioning. This study demonstrates that our data-based decomposition shows promise as it globally produces more robust results than an image-based material decomposition. Future direction involves extending the method to helical scanning and the investigation to other challenges affecting reproducibility such as physiologic motion and imaging with contrast agent.

REFERENCES

- [1] Haase, V., Hahn, K., Schöndube, H., Stierstorfer, K., Maier, A., and Noo, F., “Image reconstruction from real dual energy CT data using an analytical energy response model,” in *[2021 IEEE Nuclear Science Symposium and Medical Imaging Conference (NSS/MIC)]*, IEEE (2021).
- [2] Ren, L., Allmendinger, T., Halaweish, A., Schmidt, B., Flohr, T., McCollough, C. H., and Yu, L., “Energy-integrating-detector multi-energy CT: Implementation and a phantom study,” *Medical physics* **48**(9) (2021).
- [3] NIST, “National Institute of Standards and Technology: X-ray table.” <https://www.nist.gov/pml/x-ray-mass-attenuation-coefficients>. Last accessed: 2022-01-18.

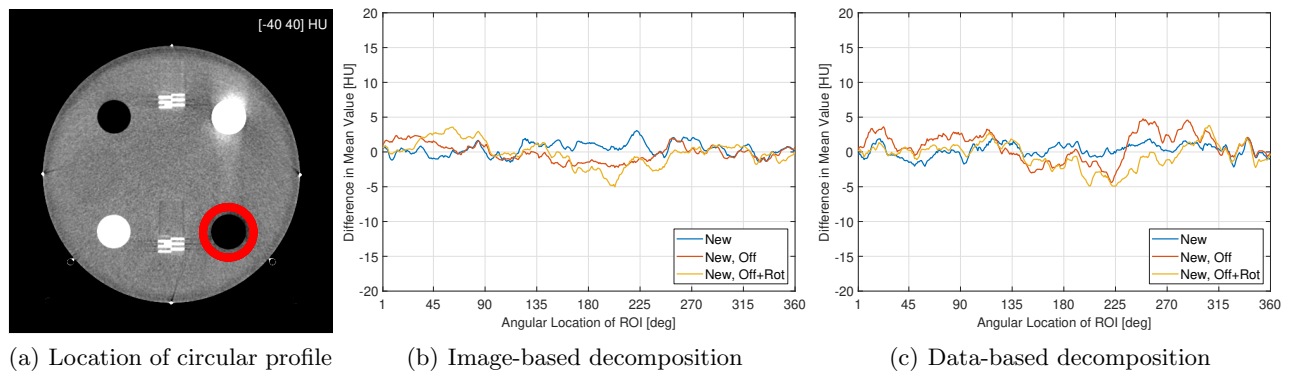


(a) Location of circular profile

(b) Image-based decomposition

(c) Data-based decomposition

Figure 5. Quantitative analysis using a circular profile plot around the bone insert. The plots show the difference in mean ROI values relative to the baseline result. The position of the ROIs is highlighted in red in the left image. The angular location of the ROIs starts at the 12 o'clock location and moves clockwise.

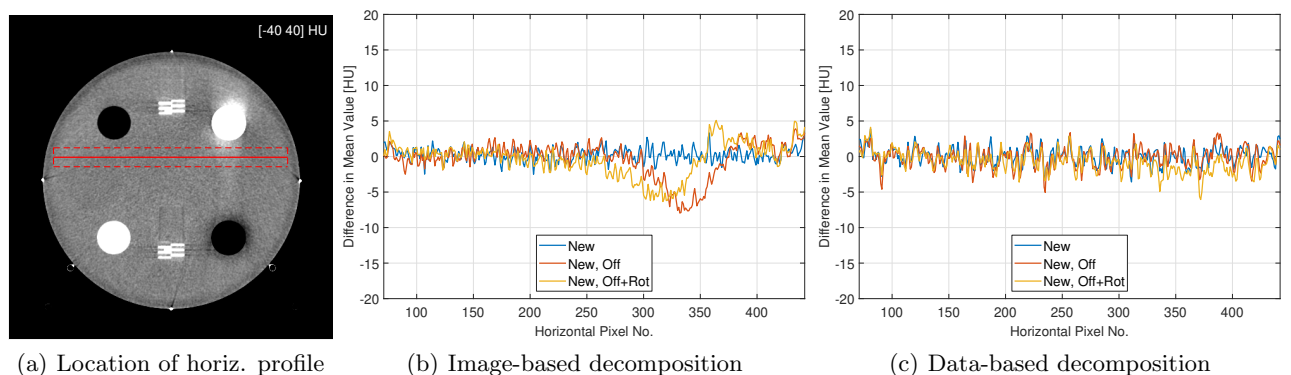


(a) Location of circular profile

(b) Image-based decomposition

(c) Data-based decomposition

Figure 6. Quantitative analysis using a circular profile plot around the air insert. The plots show the difference in mean ROI values relative to the baseline result. The position of the ROIs is highlighted in red in the left image. The angular location of the ROIs starts at the 12 o'clock location and moves clockwise.



(a) Location of horiz. profile

(b) Image-based decomposition

(c) Data-based decomposition

Figure 7. Quantitative analysis using a thick profile that averages values over 31 neighboring horizontal lines within the phantom. In the left image, the central line of the profile is marked with a solid line and the vertical range with dashed lines. The plots show the difference relative to the baseline results.